Report 317
August 2017

Application of the Analogue Method to Modeling Heat Waves: A Case Study With Power Transformers

Xiang Gao, C. Adam Schlosser and Eric Morgan

MIT Joint Program on the Science and Policy of Global Change combines cutting-edge scientific research with independent policy analysis to provide a solid foundation for the public and private decisions needed to mitigate and adapt to unavoidable global environmental changes. Being data-driven, the Joint Program uses extensive Earth system and economic data and models to produce quantitative analysis and predictions of the risks of climate change and the challenges of limiting human influence on the environment—essential knowledge for the international dialogue toward a global response to climate change.

To this end, the Joint Program brings together an interdisciplinary group from two established MIT research centers: the **Center for Global Change Science (CGCS)** and the **Center for Energy and Environmental Policy Research (CEEPR)**. These two centers—along with collaborators from the Marine Biology Laboratory (MBL) at Woods Hole and short- and long-term visitors—provide the united vision needed to solve global challenges.

At the heart of much of the program's work lies MIT's Integrated Global System Model. Through this integrated model, the program seeks to discover new interactions among natural and human climate system components; objectively assess uncertainty in economic and climate projections; critically and quantitatively analyze environmental management and policy proposals; understand complex connections among the many forces that will shape our future; and improve methods to model, monitor and verify greenhouse gas emissions and climatic impacts.

This reprint is intended to communicate research results and improve public understanding of global environment and energy challenges, thereby contributing to informed debate about climate change and the economic and social implications of policy alternatives.

—Ronald G. Prinn and John M. Reilly,
Joint Program Co-Directors

MIT Joint Program on the Science and Policy of Global Change

Massachusetts Institute of Technology
77 Massachusetts Ave., E19-411
Cambridge MA 02139-4307 (USA)

T (617) 253-7492 **F** (617) 253-9845
globalchange@mit.edu
http://globalchange.mit.edu/

GLOBAL CHANGE

AUGUST 2017

Application of the Analogue Method to Modeling Heat Waves: A Case Study With Power Transformers

Xiang Gao[1,2] C. Adam Schlosser[2] and Eric Morgan[3]

Abstract: Large power transformers (LPTs) are critical yet increasingly vulnerable components of the power grid. More frequent and intense heat waves or high temperatures can degrade their operational lifetime and thereby increase the premature failure risk. Without adequate preparedness, a widespread situation would ultimately lead to prolonged grid disruption and incur excessive economic costs. In this study, we investigate the impact of climate warming and corresponding shifts in heat waves on a selected LPT located in the Northeast corridor of the United States. We apply an analogue method, which detects the occurrence of heat waves based on the salient, associated large-scale atmospheric conditions ("composites"), to assess the risk of future change in heat wave occurrence. Compared with the more conventional approach that relies on climate model-simulated daily maximum temperature, the analogue method produces model medians of late twentieth-century heat wave frequency that are more consistent with observation and have stronger inter-model consensus. Under the future climate warming scenarios, multi-model medians of both model daily maximum temperature and the analogue method indicate strong decadal increases in heat wave frequency by the end of the 21st century, but the analogue method improves model consensus considerably. We perform a preliminary assessment on the decrease of transformer lifetime with temperature increase. Future work will focus on using more advanced algorithms to quantify the impact of more frequent heat waves on the transformer's expected lifetime and associated additional costs. The improved inter-model consensus of the analogue method is viewed as a promising step toward providing actionable information for a more stable, reliable, and environmentally responsible national grid.

1 Corresponding author (Email: xgao304@mit.edu).

2 Joint Program on the Science and Policy of Global Change, Massachusetts Institute of Technology, MA, USA.

3 MIT Lincoln Laboratory, Lexington, MA, USA.

1. Introduction

Electricity forms the backbone of nearly every modern society. It is the one sector that most other sectors depend on for their fundamental operations (Pederson *et al.*, 2006; Rinaldi, 2004). Without electricity, modern society would essentially come to a halt. This is especially true in the United States, which has arguably the most complex utility grid in the world, comprised of thousands of generation units and hundreds of thousands of miles of cables across the entire continent. The intricate electrical network is tasked with maintaining operations nearly 100% of the time, even under extreme weather conditions, shortages of fuel, direct attacks, and human errors. In the United States, prolonged disruptions in electrical service are rare, but cause widespread disorder when they do occur. Events like the Northeast blackout of 2003 (Eto, 2004), Hurricane Katrina (Select Bipartisan Committee to Investigate the Preparation for and Response to Hurricane Katrina, 2006), the California energy crisis (Federal Energy Regulatory Commission, 2003), and Hurricane Sandy (Hurricane Sandy Rebuilding Task Force, 2013) enunciate the problem. During each of these events, electricity was either disconnected or unreliable for extended periods of time, making communications, transportation, sanitation, and public safety vulnerable. Much work and thought has been dedicated to modernizing the grid to make it more resilient to weather related outages, or to terrorist attacks. Indeed, the US government is treating the utility grid as a critical asset and a national security issue (President's Council of Economic Advisers *et al.*, 2013; National Research Council, 2012; Davis and Clemmer, 2014).

Climate change is considered a direct threat to the security of the utility grid (United States Government Accountability Office, 2014; Zamuda *et al.*, 2013; van Vliet *et al.*, 2012), and can manifest itself in many ways including flooding (Bromirski *et al.*, 2012; Sathaye *et al.*, 2012), wildfires (Davis and Clemmer, 2014), more intense heat waves (Melillo *et al.*, 2014), reduced freshwater availability (Averyt *et al.*, 2011), and increased cooling water temperature (Macknick *et al.*, 2012; Fleischli and Hayat, 2014). Some of the most important yet vulnerable components of the power grid are voltage transformers (Parfomak, 2014; US DOE, 2012). Transformers are tasked with advantageously boosting or decreasing voltage for transmission so that losses are minimized. For this study, we focus our assessment of impacts from changing heatwaves on a subset of the entire network of transformers, namely, "Large Power Transformers" (LPTs)—which are transformers rated at or above 100 mVA (mega Volt-Amps). There are thousands of such LPTs across the United States. Moreover, the existing stock of LPTs is old, with 70% or more being 25 years or older out of an expected lifetime of 40 years (US DOE, 2015). Added to the burden of overhauling the aging LPT network is the fact that there are very few LPT manufacturers—and many are outside the U.S. and/or overseas. The Department of Homeland Security identified LPTs as a major bottleneck and initiated a program to research and develop temporary recovery transformers (RecX) (The Electric Power Research Institute, 2014). While strategies are being developed to modernize the utility grid, the aging fleet is increasingly vulnerable. One of the failure modes of transformers is over-heating, which degrades the electrical paper insulation within the LPT and causes catastrophic short circuits. The failure rate is more pronounced as temperature increases, due to more intense chemical reactions that age the insulation.

Climate change is expected to increase averaged temperature and produce more intense heat waves in many areas of the United States (Melillo *et al.*, 2014). All of these factors can lead to higher consumer demand for electricity, which stresses the already vulnerable fleet of LPTs beyond their design specifications. It is therefore important to assess the potential for warmer temperatures and increased heat waves and their associated impacts on LPTs in the coming decades. Currently, studying possible future changes in warm extremes generally employs various indices based on daily maximum temperature simulated with global coupled ocean-atmosphere general circulation models (CGCMs) forced with projected greenhouse gas and aerosol emissions (Kharin *et al.*, 2007, 2013; Sillmann *et al.*, 2013a,b; Russo *et al.*, 2014; Schoetter *et al.*, 2015). Some of these studies suggest that CGCMs within the Coupled Model Intercomparison Project Phase 5 (CMIP5, Meehl *et al.*, 2005) are generally able to simulate the observed warm days (Sillmann *et al.*, 2013b) or number of heat waves (Schoetter *et al.*, 2015), while others show that the models are not able to represent the number and geographical pattern of heat waves as found in the reanalysis, particularly in Europe and the U.S. (Russo *et al.*, 2014). Therefore, there is a need for a methodology that can improve the consensus among model projections and provide more actionable information for stakeholders to prepare for consequences of climate change.

In light of these considerations, we adopt an "analogue" approach that is based upon identifying the salient ingredients of observed large-scale atmospheric patterns associated with the hotter or the hottest recorded dates. In previous work, we have successfully implemented this approach to detect the occurrence of heavy and extreme summer and winter precipitation over selected areas of the United States (Gao *et al.*, 2014, 2017). The method creates composites to associate prevailing synoptic atmospheric conditions with extreme events at a local scale. In particular, when these composites are applied to an

ensemble of CMIP5 twentieth-century climate model simulations, more consistent multi-model median of heavy precipitation frequency with observation and a stronger model consensus is achieved compared to using model-simulated precipitation. However, it has not been assessed whether such an approach will yield similar performance for "heat wave" events. Toward the goal of assessing risk from future heat waves, we prototype this method to detect and predict heat wave occurrence at an LPT location in the Northeast corridor of the United States.

First, we describe the procedure for building composites of synoptic-scale upper air daily anomaly circulations that are thermodynamically associated with the "hot" days at a transformer location through a joint analysis of station-based surface daily maximum temperature observations and gridded, daily atmospheric reanalysis data. We then diagnose, calibrate, and evaluate these composites as a predictive analogue for the occurrence of a "heat wave" event. Lastly, using CMIP5 simulations we examine the performance of this analogue approach in reproducing present day heat-wave occurrence against observation as compared to estimates based on model-simulated daily maximum air temperature. Projected changes in the heat wave occurrence in response to different CMIP5 anthropogenic forcing scenarios are also examined. From these, we provide insights on the economic/cost implications on LPTs from more frequent heat waves.

The paper is organized as follows. Section 2 discusses the electrical system in the United States, the network analysis used to determine meaningful components within the grid, and the final selection of transformers based on *betweenness*. Section 3 describes the datasets (observations, reanalysis, and climate model simulations). The development, calibration and evaluation of the analogue predictive performance for heat wave occurrence are given in Section 4. In sections 5 and 6 we discuss the comparative performance of the analogue scheme against simulated daily maximum temperature when applied to CMIP5's late 20th century historical climate as well as future climate under two radiative forcing scenarios, respectively. Section 7 discusses the threat of premature failure in LPTs and potential costs associated with future changes in heat wave frequency. Summary and discussions are provided in Section 8.

2. Transformer Selection

Electrification is listed by the National Academy of Engineering as the greatest achievement of the 20th century (Constable and Somerville, 2003). Indeed, the United States is home to one of the largest connected networks of machines on the planet, consisting of over 50,000 substation locations and connected by over 200,000 miles of transmission lines (Eto, 2004). **Figure 1** shows the basic layout of the electrical system, beginning with the generation of power and step-up voltage conversion, followed by transmission over large distances, then by step-down voltage conversion. The extreme voltages are employed to minimize power loss, which increases as the square of current.

Given the immensity of the electrical grid, determining key components is a challenging task. Here we employ graph theory, also known as network analysis, to select meaningful transformers in the Northeastern United States. Network analysis treats the physical topology of electrical grid as a series of nodes (transformers) and edges (transmission lines) so that basic mathematical analysis can be performed. The mathematics range from simple metrics like the degree of a node (Newman, 2010), meaning how many connections it has, to the "betweenness centrality" of a node—a measure of the network's connectivity (Barthelemy, 2004). In this work, we chose to use betweenness to select transformers since high betweenness has been shown to be a meaningful parameter

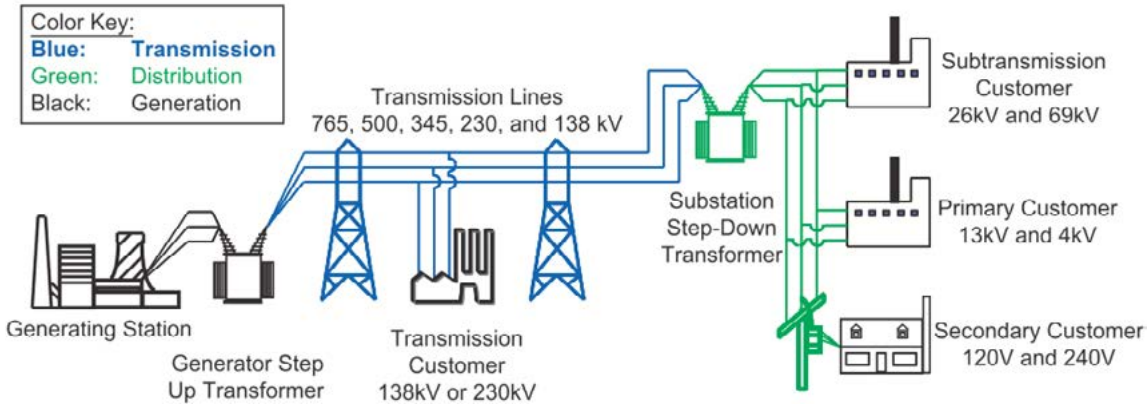

Figure 1. Generation, Transmission and Distribution Systems in the US (Eto, 2004).

for cascading failures in the North American power grid (Kinney *et al.*, 2005; Albert *et al.*, 2004; Bompard *et al.*, 2010). While a discussion of betweenness is beyond the scope of this work, the concept is presented in **Figure 2**. Here, two networks (Region I and Region II) are connected by a single point, T. Thus, all flows between Region I and Region II must utilize T. Severing T will result in two independent regions. Formally, the betweenness of any node v measures the fraction of shortest paths flowing through that node (Barthelemy, 2004), or:

$$g(v) = \sum_{s \neq v \neq t} \frac{\sigma_{st}(v)}{\sigma_{st}}$$

where σ_{st} is the total number of shortest paths between nodes s and t and $\sigma_{st}(v)$ is the total number of shortest paths from s to t via v.

We focus the network analysis on the electrical grid in the Northeastern United States. For simplicity, and to prove the overall concept, we use just the transformers and transmission lines. We omit the generation plants, the distribution lines, and any nodes or edges that are disconnected from the larger system. The final analysis results in 3839 transformers (nodes) connected with 4770 edges (transmission lines). We assume lines to be "undirected", that is power could flow in any direction on the lines. Each transformer is found to, on average, be connected to 2.485 lines. The average path length between two nodes is found to be 18.133, meaning that, on average, more than 18 other nodes are on the path between any two random nodes. We calculate the betweenness centrality for each of the 3839 nodes in the network and create a topological connectivity map, shown in **Figure 3**. The nodes are sized and colored according to their betweenness centrality, with large, green nodes having high betweenness. The lowest betweenness nodes are depicted as small, red dots. We select the top twenty highest betweenness nodes for our analogue method analysis.

3. Datasets

3.1 Observed Daily Maximum Air Temperature

The Global Historical Climatology Network-Daily (GHCN-Daily) (Menne *et al.*, 2012) is comprised of approximately 27,000 stations globally with daily maximum and minimum temperature. GHCN-Daily is composed of daily weather reports from numerous sources that have been merged and subjected to a common suite of quality assurance (QA) reviews. The maximum temperature data from the stations close to the transformers will be used to identify the observed heat wave days.

3.2 NASA MERRA-2 Reanalysis

We employ Modern Era Retrospective-analysis for Research and Applications Version 2 (MERRA-2, Bosilovich *et al.*, 2016) to analyze the large-scale atmospheric circulations associated with our targeted extreme heat events, and for calibration and evaluation. In comparison with the MERRA dataset used in the previous studies (Gao *et al.*, 2014, 2017), MERRA-2 represents the advances made in both the Goddard Earth Observing System Model, Version 5 (GEOS-5) and the Global Statistical Interpolation (GSI) assimilation system that enable assimilation of modern hyperspectral radiance and microwave observations, along with GPS-Radio Occultation datasets. MERRA-2 is the first long-term global reanalysis to assimilate space-based observations of aerosols and represent their interactions with other physical processes in the climate system. The MERRA-2 is updated in real time, spanning the period from 1980 to the present. The three-dimensional 3 hourly atmospheric diagnostics on 42 pressure levels are available at a 0.625° × 0.5° resolution.

3.3 Climate Model Simulations

We use the climate model simulations from the CMIP5 historical experiment (years 1850–2005) and experiments for the 21st century (years 2006–2100) employing

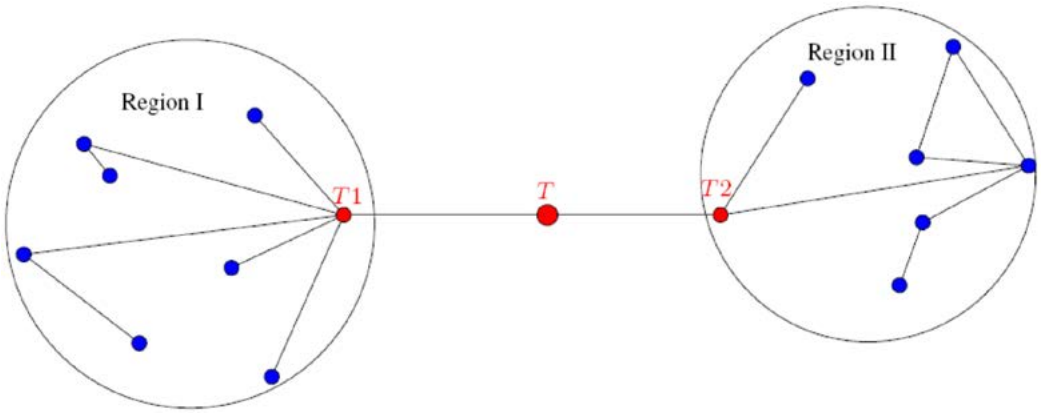

Figure 2. Node T has high betweenness even though it has few neighbors. Removing T serves the network into two disjoint components.

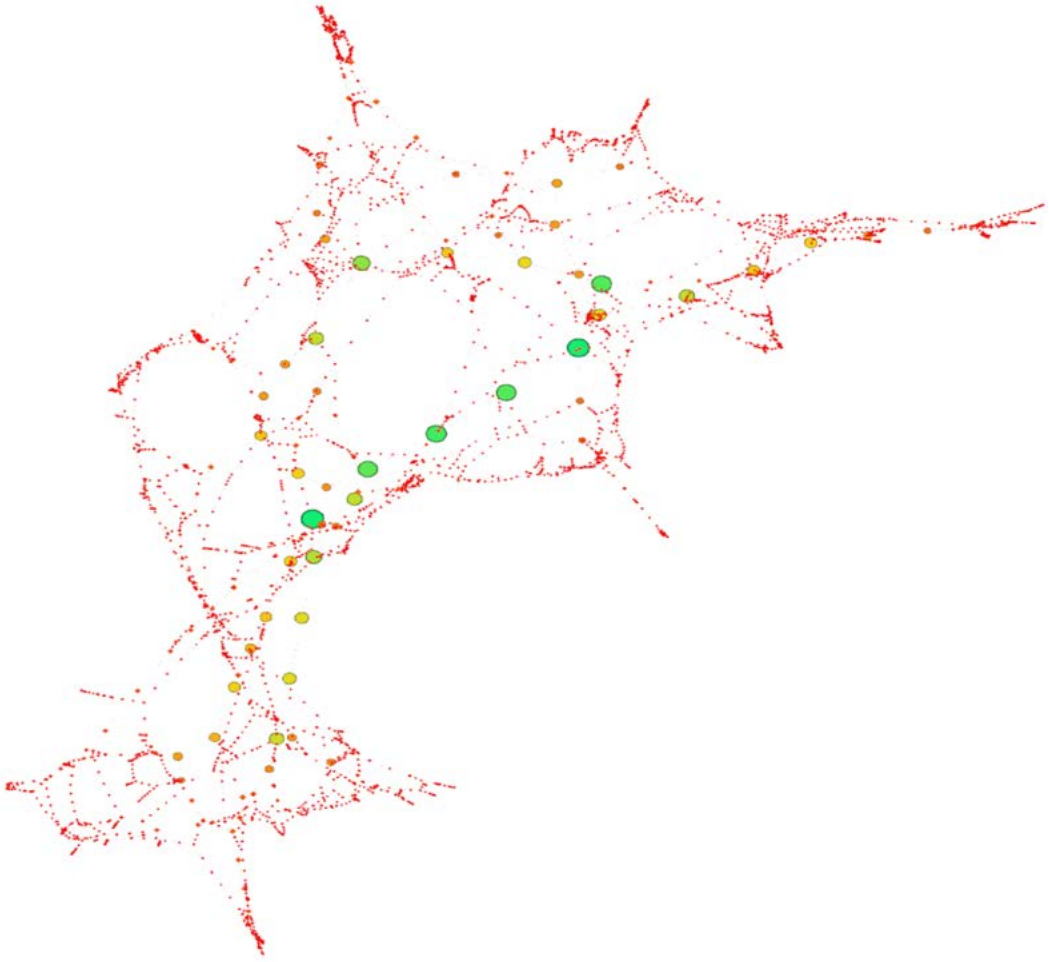

Figure 3. Northeast US electrical grid network representation using "Betweenness".

two different radiative forcing scenarios. The historical runs were forced with observed temporal variations of anthropogenic and natural forcings and, for the first time, time-evolving land cover (Taylor *et al.*, 2011). The future scenarios, called Representative Concentration Pathways (RCPs, Moss *et al.*, 2010), are designed to accommodate a wide range of possibilities in social and economic development consistent with specific radiative forcing paths. The estimated radiative forcing values by year 2100 are 4.5 W/m^2 and 8.5 W/m^2 in the two experiments considered here, namely RCP4.5 and RCP8.5. A total of 20 models provide all the essential meteorological variables for the analogue scheme across the three experiments considered here (**Table 1**). In this study, only one ensemble member from each model is analyzed.

3.4 Data Processing and Analyses

The same set of meteorological variables are assembled or derived from both the MERRA-2 reanalysis and climate model simulations, including 500hPa vector winds (*u500* and *v500*), 500hPa vertical pressure velocity (*w500*), 500hPa vorticity (*epv500*), and vertically integrated enthalpy (*cpt*). The 3-hourly MERRA-2 atmospheric diagnostics are first averaged into daily. All the daily fields, including the daily maximum air temperature and meteorological fields from MERRA-2 reanalysis and each CMIP5 climate model, are then regridded to a common 2.5° × 2° resolution via area-weighted averaging. The period with the greatest overlap among the GHCN station data, MERRA-2 reanalysis, and CMIP5 historical experiment is 1 January, 1980–31 December, 2002. So at each grid cell, we convert the meteorological fields of each data source to normalized anomalies based on their respective seasonal climatological mean and standard deviation of this 23-yr period. The same seasonal climatological means and standard deviations are also employed to obtain the normalized anomalies for the meteorological fields of MERRA-2 reanalysis from 2003 to 2006 and CMIP5 two RCP experiments from 2006 to 2100. The MERRA-2 reanalysis large scale atmospheric fields from 1980 to 2002 will be used to develop and calibrate the analogue scheme, and from 2003 to 2006 as a provisional validation period.

We use the GHCN station data to identify the observed heat wave days at the transformer of our interest, while

Table 1. List of the CMIP5 models used for analysis in this study.

Model Name	Country	Resolution	Run	Institution
ACCESS1-0	Australia	192x144L38	1	Commonwealth Scientific and Industrial Research Organization, and Bureau of Meteorology
ACCESS1-3	Australia	192x144L38	1	Commonwealth Scientific and Industrial Research Organization, and Bureau of Meteorology
BCC-CSM1-1	China	128x64L26	1	Beijing Climate Center, China Meteorological Administration
BCC-CSM1-1-m	China	320x160L26	1	Beijing Climate Center, China Meteorological Administration
BNU-ESM	China	128x64L26	1	College of Global Change and Earth System Science, Beijing Normal University
CanESM2	Canada	128x64L35	5	Canadian Centre for Climate Modelling and Analysis
CCSM4	USA	288x192L26	1	National Center for Atmospheric Research
CMCC-CM	Italy	480x240L31	1	Centro Euro-Mediterraneo per I Cambiamenti Climatici
CNRM-CM5	France	256x128L31	1	Centre National de Recherches Meteorologiques
GFDL-CM3	USA	144x90L48	1	Geophysical Fluid Dynamics Laboratory
GFDL-ESM2G	USA	144x90L24	1	Geophysical Fluid Dynamics Laboratory
GFDL-ESM2M	USA	144x90L24	1	Geophysical Fluid Dynamics Laboratory
IPSL-CM5A-LR	France	96x96L39	6	Institut Pierre-Simon Laplace
IPSL-CM5A-MR	France	144x143L39	3	Institut Pierre-Simon Laplace
IPSL-CM5B-LR	France	96x96L39	1	Institut Pierre-Simon Laplace
MIROC5	Japan	256x128L40	5	Atmosphere and Ocean Research Institute, National Institute for Environmental Studies, and Japan Agency for Marine-Earth Science and Technology
MIROC-ESM-CHEM	Japan	128x64L80	1	Japan Agency for Marine-Earth Science and Technology, Atmosphere and Ocean Research Institute, and National Institute for Environmental Studies
CSIRO-MK3.6	Australia	192x96L18	10	Commonwealth Scientific and Industrial Research Organization/Queensland Climate Change Centre of Excellence
MRI-CGCM3	Japan	320x160L48	1	Meteorological Research Institute
NorESM1-M	Norway	144x96L26	3	Norwegian Climate Centre

the MERRA-2 reanalysis is employed to construct the large-scale composites of atmospheric patterns associated with identified heat wave days, and to calibrate and evaluate the analogue scheme. We are interested in: 1) the extent to which the analogue method matches or exceeds the performance of MERRA-2 daily maximum air temperature in identifying observed heat wave occurrences; 2) the extent to which the analogue method improves upon CMIP5 model-simulated daily maximum air temperature in terms of detecting the cumulative heat wave occurrences under contemporary climate and their changes as climate warms.

4. Calibration and Evaluation of Analogue Method

Currently, there is no universally appointed or accepted definition of a "heat wave" event. A comprehensive survey of the total body of research in this area is well beyond the scope of this research, yet several of the more recent definitions are presented in Grotjahn (2011, See Table 1). These definitions include such considerations as consecutive days above a threshold value or percentile and combinations thereof. Many among these types of metrics are designed with the consideration of a prolonged exposure of "excessive" heat. In this study, the stress from excessive heat on an LPT does not necessarily need to be from a prolonged event (i.e. multiple, consecutive days) and is also more directly associated to exceedance of an absolute temperature (average and/or daily maximum) rather than a more meteorologically-based metric tied to a percentile exceedance. High temperatures affect the peak load capability of an LPT, which can decrease by about 10% at extreme temperatures (Sathaye, 2011; Li *et al.*, 2005) and increase the risk of transformer failure (He *et al.*, 2009; Weekes *et al.*, 2004; Fu *et al.*, 2001), while reducing the operational lifetime (Askari *et al.*, 2009). In this context, we are interested in the deterioration of an LPT associated with a preponderance of days—and anticipated trends in the coming decades—whose temperatures reach or exceed what are incrementally damaging as a result of ambient conditions and/or load burdens from electricity demands. Given the above considerations and for the purposes of this pilot study, we define a "heat wave" as a day in which the daily maximum temperature is at or exceeds 90°F (or ~32°C)

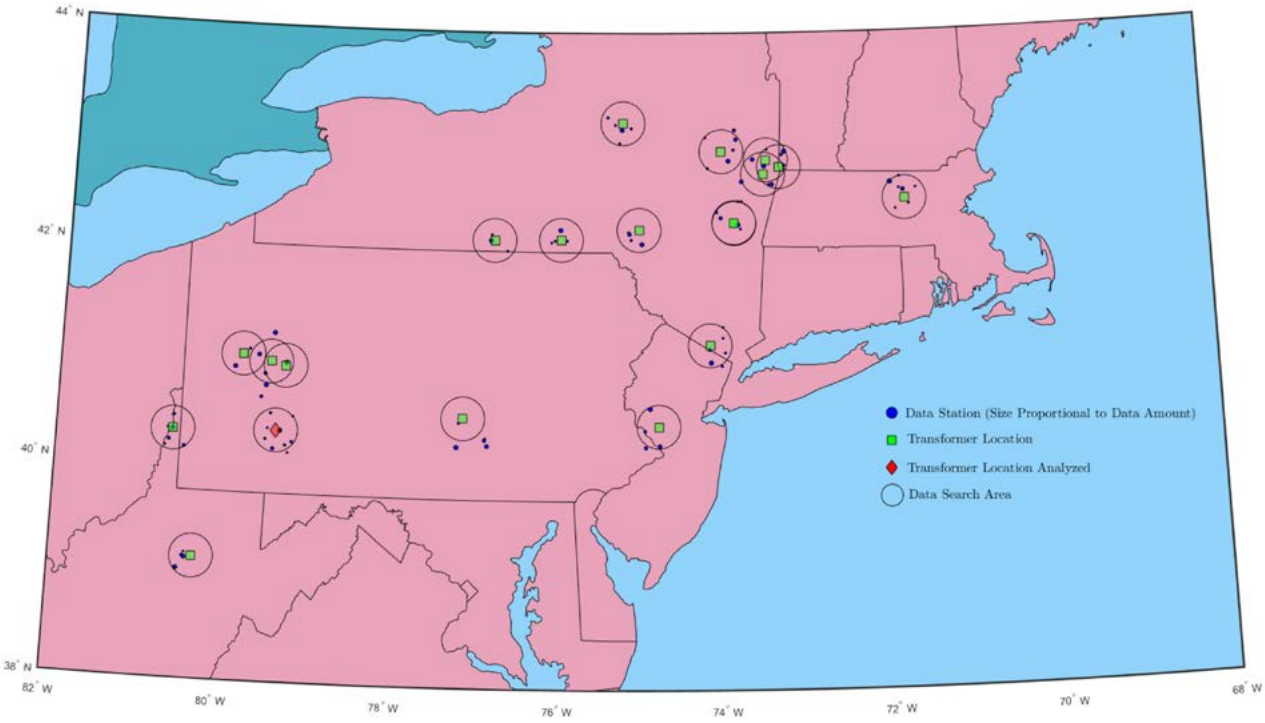

Figure 4. Locations of transformers and weather stations.

at an observation station or model grid. The selection of a 90°F threshold is further justified below by also considering the impact of humidity.

On the basis of our aforementioned network analysis of transformers over the Northeast U.S. (Section 2), we performed additional analysis for the high betweenness LPTs we identified (Figure 3) to assess: 1) availability of nearby GHCN meteorological observations and; 2) the occurrence of heatwave events—as we have defined—over the period of each observational record in order that they can serve as strong candidates for this pilot study. From this, we found an LPT located in southwest Pennsylvania (**Figure 4**, denoted by the red diamond). Within a 0.5° radius of the transformer, 7 GHCN stations with daily maximum temperature observations are available. We have selected two of these stations that contained the longest records (20+ years of data) and located at an elevation that is close (within 10s of meters) to that of the LPT. The common heat wave dates from two these stations are then used to identify observed heat wave dates.

Looking at this LPT location, our selection of a 90°F threshold is further justified by also considering the impact of humidity. For air temperatures exceeding 90°F, its corresponding heat index will exceed 95°F at dew point temperatures equal to or greater than 67°F. Although the GHCN stations do not contain dew point temperatures as part of the archived data, we can use the daily minimum temperature data as an approximation for dew point temperature, noting that there are certain conditions when this estimate may be limited (Williams *et al.*, 2015). Upon pooling the minimum temperature data for only the days in which the maximum temperature is equal to or exceeding 90°F, we find that for 20%–30% of those days the dew point is at or above 67°F (**Figure 5**). In these situations, the transformers would most likely be additionally burdened by electrical demands associated with HVAC cooling.

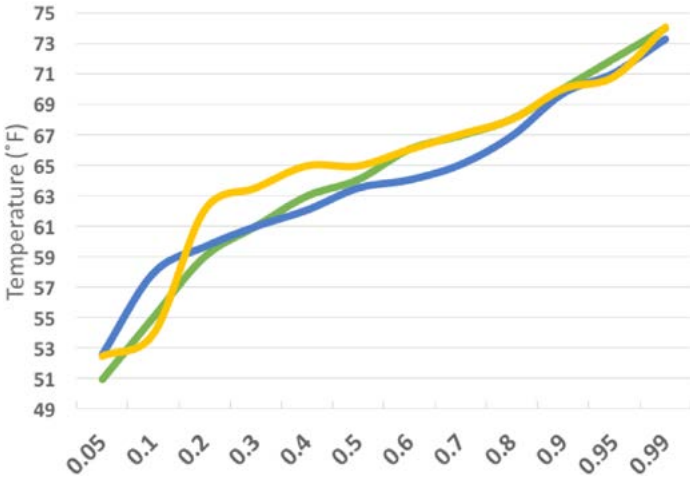

Figure 5. Cumulative distributions of the estimated (daily) dew point temperature for three of the GHCN stations in proximity to the T2 transformer location. The distributions are constructed by pooling only the days in which the daily maximum temperature is equal to or greater than 90°F.

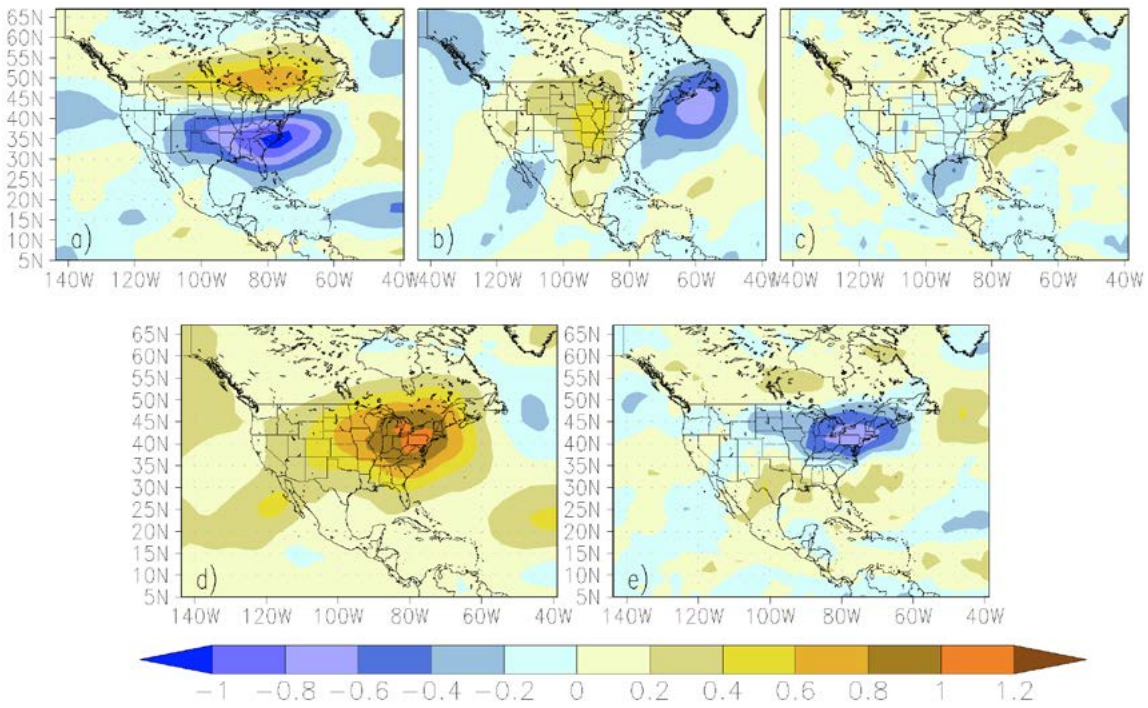

Figure 6. Composite fields as normalized anomalies at 2.5° × 2° for the transformer T2 in JJA: a) 500hPa zonal velocity (u_{500}); b) 500hPa meridional velocity (v_{500}); c) 500hPa vertical pressure velocity (w_{500}); d) vertically integrated enthalpy; and e) 500hPa vorticity (epv_{500}) based on 157 heat wave days.

4.1 Synoptic Condition Composites

We extract 157 heat wave days from the GHCN observations of 1980–2002 for the June-August (JJA) season. We examine various atmospheric fields, which provide insight into the preferred synoptic conditions conducive to the heat wave. **Figure 6** shows the composites as standardized anomalies, produced by averaging the MERRA-2 reanalysis atmospheric anomaly fields across the observed heat wave days. The composites indicate that heat wave or the hotter days are associated with: large-scale anticyclonic circulation at the mid-levels of the atmosphere (Fig. 6a,b); usually warm lower tropospheric temperature (at 850 hPa, not shown); and corresponding anomalous positive enthalpy (Fig. 6d) over the transformer area. Also evident are the negative anomalous vorticity (Fig. 6e) over the region and the presence of sinking air to the east and off the coast of the Carolinas that also extends eastward across the Bermuda Islands (Fig. 6c). This large sinking region of air is consistent with the location of the classic "Bermuda High" surface-pressure system, and the associated circulation supports the advection of warm near-surface air from the Gulf of Mexico that is spread across the eastern seaboard of the United States.

4.2 Analogue Detection Diagnostics

Here all the composite variables, including 500hPa zonal and meridional wind (u_{500} and v_{500}), 500hPa vertical velocity (w_{500}), 500hPa vorticity (epv_{500}), and vertically integrated enthalpy (cpt) are used to construct the analogue scheme for detecting the occurrence of a heat wave. 500hPa geopotential height is not used because it was found in (Gao *et al.*, 2017) that their overall increasing trend associated with climate warming disrupts the anomalous dipole structure with respect to current climate conditions, making its application in analogue method for future climates problematic. In contrast, the distinct patterns of normalized anomaly composites of horizontal wind vector components were fairly well preserved between the current and future climates. The synoptic behaviors exhibited by the other composite variables were also found to be fairly consistent between the contemporary and projected climates (not shown). This would suggest that it is reasonable to expect that there will be no adverse trends in the normalized anomaly patterns of these atmospheric variables associated with the occurrence of a heat wave, and can thus be applied for assessing the heat wave frequency changes in a future climate.

We employ two metrics, "hotspot" and spatial anomaly correlation coefficient (SACC), in order to gauge whether the distinct synoptic conditions conducive to heat wave identified by the composites (Figure 6) have been replicated on any given day. The "hotspot" metric diagnoses the extent to which the composite of each at-

mospheric field is representative of any individual heat wave day. It involves the calculation of sign count at each grid cell by recording the number of individual members whose standardized anomalies have consistent sign with the composite. "Hotspots" are identified as the grid cells where the members used to construct the composites exhibit strong sign consistency with the composite itself (i.e. the larger sign counts). SACC is calculated between the MERRA-2 atmospheric fields and the corresponding composites for each day of JJA from 1980 to 2002. The exact region used for SACC calculation is arbitrary, but its boundaries are chosen such that the coherent structures of the composite fields are captured and centered. We then assess ten ranges of SACC thresholds from 0.0 to 1.0 with an interval of 0.1. We test the SACC calculations for regions with small differences in their size and aspect ratio, but find that the resulting optimal thresholds (described later) are insensitive to these differences for the analogue scheme.

We follow the similar "criteria of detection" for the analogue scheme in Gao *et al.* (2014, 2017), but relax them due to the use of more variables in this study by treating two horizontal wind components as two variables corresponding to the trough and ridge of geopotential height and adjusting the cut-off number for each metric. The criteria are: 1) At least 4 out of 5 variables have consistent signs with the corresponding composites over the selected "hotspot" grid cells; 2) at least 3 out of 5 variables has SACC larger than the determined thresholds.

4.3 Calibration and Evaluation

We employ automatic calibration to determine the cut-off values for the number of hotspots and thresholds for SACC of all five atmospheric fields simultaneously. The calibration is performed by running different combinations of the number of hotspots and ranges of SACC values across all atmospheric fields, and assessing the daily MERRA-2 atmospheric fields in JJA from 1980 to 2002 to determine whether the "criteria of detection" described above is met for that day. If so, the day is considered as having a heat wave occurring. We use the "confusion matrix" commonly employed in the binary classification as goodness-of-fit criteria to evaluate how well the analogue scheme reproduces the observed heat wave days. The same measures are also employed to assess how well the analogue scheme with optimized threshold values apply for the independent MERRA-2 reanalysis from year 2003 to 2006, compared to the observed and MERRA-2 daily maximum temperature-based analyses.

Confusion matrix features four values, namely, the number of true positives (TP), false positives (FP, type I error), true negatives (TN), and false negatives (FN, type II error). We employ five more metrics as performance measures derived from these four numbers:

1. True positive rate (TPR) given as TPR = TP / (TP+FN)
2. False positive rate (FPR) given by FPR = FP / (FP+TN)
3. Precision or positive predictive value (PPV) given as PPV=TP / (TP+FP)
4. Accuracy (ACC) given as ACC = (TP+TN) / (TP+FP+TN+FN)
5. The F1 score is the harmonic mean of precision and true positive rate and calculated as F1 = 2×TP / (2×TP+FP+FN)

Accuracy, though widely used to evaluate the robustness of a model for making predictions, is not a reliable metric for the real performance of a classifier, because it will yield misleading results if the data set is unbalanced (that is, when the number of samples in different classes vary greatly) just like the case of heat wave versus non-heat wave days. The additional meaningful measures to evaluate such a classifier are precision and true positive rate, which can be thought of as measures of a classifier exactness and completeness, respectively. A low precision and low true positive rate indicate a large number of false positive and false negative, respectively. F1 score conveys the balance between the precision and the true positive rate. In our study, the optimal cut-off values for the number of hotspots and thresholds for SACC are achieved by producing the observed number of heat wave days (equal to TP+FP) with the best TPR. In this case, FP is equal to FN, and F1 score is equal to PPV and TPR.

Table 2 shows performance measures of using analogue scheme and MERRA-2 daily maxi- mum temperature to detect JJA heat wave during calibration (1980–2002) and validation (2003– 2006) periods. During the calibration period, the analogue scheme has slightly better performance metrics than the MERRA-2 daily maximum temperature, with higher TPR, PPV, and F1 score, slightly higher ACC and slightly lower FPR. The TPR, PPV, F1 score, ACC, and FPR are 52%, 52%, 52%, 93% and 4% for analogue scheme in comparison with 48%, 48%, 48%, 92%, and 4% for MERRA-2 daily maximum temperature. During the validation period, both analyses strongly overestimate the number of heat wave days, but the performances of MERRA-2 daily maximum temperature are better than those of analogue scheme. The TPR, PPV, F1 score, ACC, and FPR are 64%, 25%, 36%, 93% and 6% for analogue scheme in comparison with 91%, 39%, 54%, 95%, and 5% for MERRA-2 daily maximum temperature. Note that MERRA is not purely model-based, but assimilates a number of observations—primarily states, motions, and transport in the atmosphere throughout both periods. In contrast, the analogue scheme is applied to the data of the validation period that is completely in-

Table 2. Calibration and validation statistics with the use of five atmospheric variables to construct analogue diagnostics for JJA of transformer T2. FNR and TNR are not included in the table as they can be simply derived from TPR and FPR, respectively. The numbers highlighted in light gray indicate the better performance in analogue than in MERRA daily maximum air temperature. The numbers highlighted in dark gray indicate the total number of observed heat wave days.

Scheme	TPR	FPR	ACC	PPV	F1 Score	Total Events
1980–2002 (157)						
MERRA-2	0.484	0.042	0.922	0.478	0.481	159
uvw_epv_cpt	0.516	0.039	0.928	0.516	0.516	157
2003–2006 (11)						
MERRA-2	0.909	0.045	0.954	0.385	0.541	26
uvw_epv_cpt	0.636	0.059	0.932	0.250	0.359	28

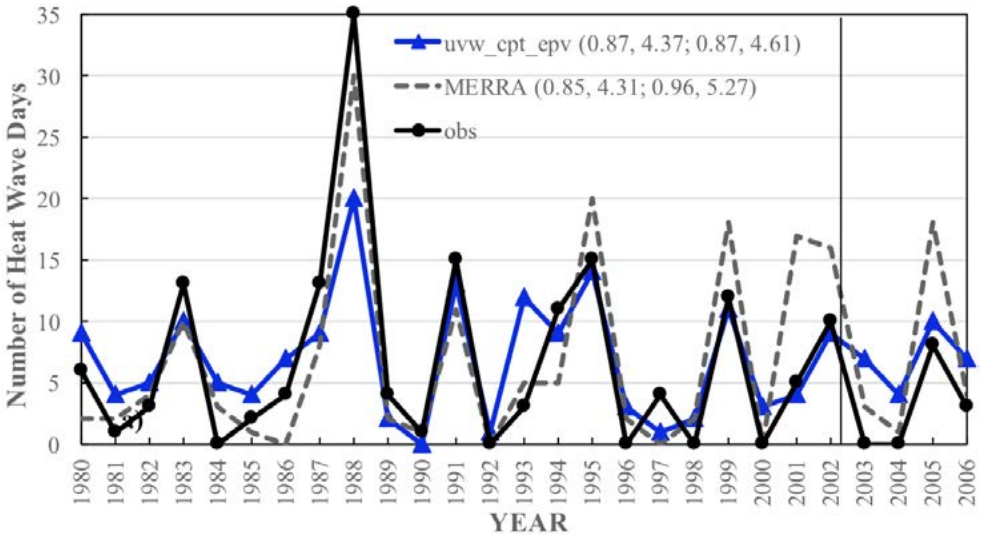

Figure 7. Comparisons of interannual variations of seasonal heat wave frequency obtained from analogue scheme, MERRA-2 daily maximum air temperature (MERRA-2), and the observation (obs) for JJA during the calibration (1980–2002) and validation (2003–2006) period. Also shown in the parentheses of figure legend are temporal correlations and RMSE between various schemes and observation during two periods.

dependent from the training data used for tuning their parameters. Since MERRA is considered to be as close to a global gridded observational dataset as one can find, it is not surprising that it performs well, or outperforms the analogue scheme in some cases. The FPRs and ACCs are fairly insensitive measures with only minor changes. Little changes in ACC values across two periods and two analyses (MERRA-2 daily maximum temperature versus analogue scheme) are mostly attributed to our unbalanced data set with non-heat wave days (and thus TN) occupying the large portion, while little changes in FPR values are associated with both the dominance of TN and the same order of detected total heat wave days (and thus FP) by two analyses. Worthy to note is that the statistics of performance measures during the validation period may not be robust due to relatively short record length.

We also examine the performances of analogue scheme in depicting the interannual variations of JJA heat wave frequency from 1980 to 2002 (calibration) and 2003 to 2006 (validation) as opposed to the station observation and MERRA-2 daily maximum temperature at 2.5° × 2° (**Figure 7**). The analogue scheme and MERRA-2 daily maximum temperature reproduce the observed interannual variations of summer heat wave frequency reasonably well with the temporal correlation above 0.85 and a root mean square error (RMSE) of about 5 days during both periods. Two analyses exhibit the similar correlations and RMSEs. More specifically, we find that both analyses capture more salient multi-year peaks, such as the heat waves that occurred in 1983, 1988, 1991, 1995, 1999, 2002 and 2005 as well as valleys in 1990, 1992, 1996, 1998, and 2000. MERRA-2 daily maximum temperature overestimates the observed number of heat wave days for the summer of 1995, 1999, 2001, 2002, and 2005, but underestimates that for the summer of 1988 and 1994. The analogue scheme strongly underestimates the observed number of heat wave days for the summer of 1988, but overestimates that for the summer of 1993, 2003, and 2004.

5. Simulated Late 20th Century Heat Wave Frequency

Next we apply the analogue scheme to the CMIP5 late 20th century model simulations. We examine the capabilities of current state-of-the-art climate models to realistically replicate the "resolved" large-scale atmospheric conditions associated with heat wave. Evaluating the circulation behaviors linked to the occurrence of heatwave events in climate models under contemporary climate can ensure the assessment of their future changes with greater confidence. This is achieved by judging the CMIP5 model-simulated daily meteorological conditions of 1980 to 2002 against the constructed composites (e.g. Figure 6) for their similarity in terms of the established "criteria of detection" (described in Section 4.2). In this way, any day when the "criteria of detection" are met would be considered as a heat wave day. We then compare the results of the analogue scheme with those identified from the station observation, MERRA-2 and CMIP5 model daily maximum temperature at 2.5° × 2° resolution.

Figure 8 displays the comparisons of the number of 1980–2002 summer heat wave days obtained from the CMIP5 model daily maximum temperature and analogue scheme across 20 climate models. Also included is the number of heat wave days estimated from the station observation (the result from MERRA-2 daily maximum temperature is very close to that of the observation, so is not included). Strikingly evident is that the daily maximum temperature-based analyses (the "tasmax" whisker plot) from all the models exhibit a wide degree of estimation and the resulting heat wave frequencies demonstrate a wide inter interquartile range (IQR, ≈450 days) and inter-model spread (≈1035 days). More models tend to underestimate the number of heat wave days with the multi-model median below the observation. In contrast, the results from the analogue scheme produce more consistent multi-model medians with the observation as well as much reduced IQRs (≈80 days) and inter-model ranges (≈160 days). The central tendency of the analogue scheme slightly overestimates the number of heat wave days with the observation falling just below the multi-model median. Overall, the analogue scheme improves upon the model daily maximum temperature in terms of their assessment of late 20th century heat wave frequency from the perspectives of both accuracy (consistencies of multi-model medians with observation) and precision (inter-model spreads). This demonstrates that state-of-the-art climate models are capable of reproducing the atmospheric synoptic conditions associated with heat wave with realistic frequency. Accordingly, the analogue scheme based on resolved large scale circulation features presents collectively better skill in identifying the observed cumulative heat wave occurrence compared to estimates from model-simulated daily maximum surface-air temperature.

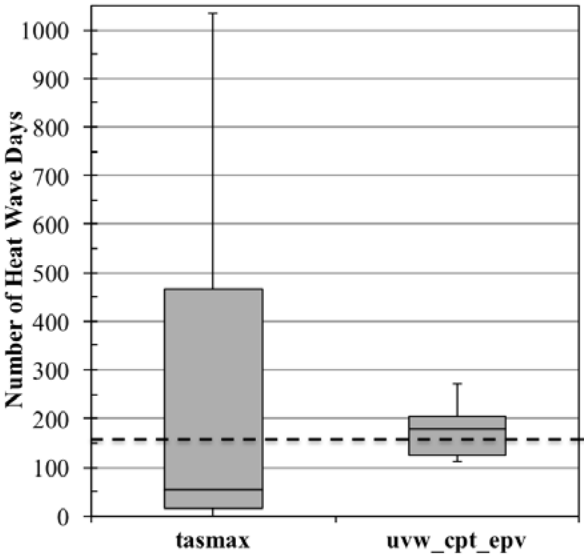

Figure 8. Comparisons of the number of summer season (JJA) heat wave days estimated from CMIP5 model-simulated daily maximum air temperature and analogue scheme applied to CMIP5 model-simulated atmospheric synoptic conditions during the period of 1980 to 2002. The whisker plot shows the minimum, the lower and upper quartile, median, and the maximum across 20 CMIP5 models. The dashed indicates the number of heat wave days identified from the GHCN station and MERRA-2 daily maximum air temperature at 2.5°× 2°. The 90°F is used to extract heat wave days for all the data sources.

6. Projected Future Changes in Heat Wave Frequency

Given the results from the late 20th century assessment, we apply the method to assess the heat wave occurrence in the CMIP5 models from the RCP experiments from 2006 to 2100. The use of fixed thresholds is one of the ways to examine how the predefined events (i.e. heat wave) migrate in a changing climate. We convert the CMIP5 model-simulated daily meteorological fields from 2006 to 2100 to normalized anomalies relative to the seasonal climatological means and standard deviations of each model from the CMIP5 historical simulations (1980–2002). We analyze the projected changes in heat wave frequency between the 23-year period of 2070 to 2092 and 2010 to 2032. The relative change is expressed as number of days per year. This is done for both model-based daily maximum temperature and the analogue scheme.

Figure 9 displays the changes in heat wave frequency estimated from an ensemble of model daily maximum temperature and the analogue scheme under RCP8.5 and 4.5 scenarios. Under the RCP8.5 scenario, the multi-model medians of both analyses indicate pronounced increases in heat wave frequency, with medians of both analy-

ses showing about 23 more days/year by the end of the century; this change is nearly quadruple the average number of events (~6) seen every summer through the historical period (1980–2006, see Table 2). All the models from both analyses consistently show the increases in frequency. Inter-model disagreements in the magnitude of change remain larger for model daily maximum temperature than for the analogue result, ranging from increases of 3~48 and 9~37 days per year, respectively. The analogue scheme, however, provides a much reduced IQR (≈7 days), about one-third as much as that of model daily maximum temperature (≈20 days). As expected, the increases in the heat wave frequency from both analyses are less pronounced under the lower emission scenario RCP4.5, with multi-model medians showing 8.4 more days/year for daily maximum temperature and 7.2 more days/year for the analogue scheme. However, this median result implies that even under a strong mitigation scenario the number of heat waves during JJA will be double that from the historical (1980–2006) period. The mitigation tends to shift not only the multi-model medians but also the entire distributions toward the smaller increases in heat wave frequency. Nevertheless, all the models from both analyses show consistency in the sign of change (increase). The inter-model consensuses are largely reduced due to the smaller radiative forcing, ranging from increase of 0.1–22 and 1.6–12 days per year for daily maximum temperature and analogue scheme, respectively. Likewise, the IQR of the analogue result (≈3 days) is about one third as much as that of model daily maximum temperature (≈11 days). Overall, the analogue scheme improves upon model daily maximum temperature by producing a much stronger model consensus in both emission scenarios.

7. Economic Impacts

Large power transformers (LPTs) are one of the most expensive single pieces of equipment on the electrical grid (US DOE, 2012). Failure of a single transformer can lead to widespread outages for prolonged periods of time, incurring economic costs in terms of lost wages and productivity (Sullivan *et al.*, 2015). Moreover, the manufacture and delivery of LPTs is a complicated process involving several industries and complex logistics and lead times on LPTs can be in the range of years. LPTs are vulnerable to overheating and must be monitored closely to maintain proper operating temperatures. Cooling systems for LPTs are typically oil-based convective heat sinks that circulate oil around the windings of the LPT and transfer the heat to the environment via fans. The systems are not perfect, and often develop "hot spots" within the LPT (Susa and Nordman, 2009). These hot spots can damage the insulating paper that protects the windings from short circuits. Such short circuits can severely damage the transformer and lead to sudden, catastrophic failures.

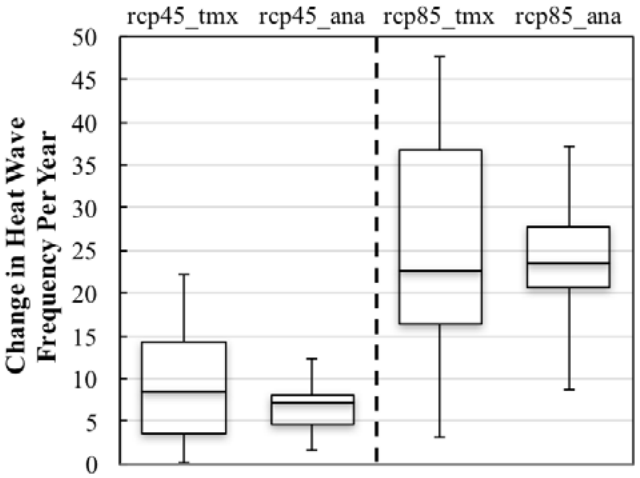

Figure 9. The changes in heat wave frequency between the period of 2070 to 2092 and the period of 2010 to 2032 estimated from an ensemble of CMIP5 model daily maximum air temperature and synoptic conditions employed by analogue schemes under RCP8.5 and RCP4.5 scenarios for JJA of transformer T2.

The cooling systems of LPTs are designed such that a threshold temperature of about 90°C—the temperature at which the insulating paper begins degradation (Godina *et al.*, 2015)—is rarely or ever exceeded. The transformer rating (in kVA) is based on a 24-hour average temperature of 30°C (IEEE, 2012), and any temperature above this value decreases the KVA rating by about 1% per degree C. The expected life of a transformer is related to the operating temperature which ages the insulating paper between the windings given by Lundgaard *et al.* (2004):

$$Expected\ Life = \left[\frac{\frac{1}{DP_{End}} - \frac{1}{DP_{Start}}}{A \times 24 \times 365}\right] \exp\left({}^{13350}/_{T}\right) \quad (1)$$

where DP_{Start} and DP_{End} are the degree of polymerization of the cellulose at the beginning (≈1000) and end of the transformer life (≈200), respectively; A is the pre-exponential factor, determined to be 2E+8, and T is the temperature in Kelvin. Assuming a design life of 40 years (Metwally, 2011; US DOE, 2012), this corresponds to a temperature of about 82°C and is close to the IEEE standard (IEEE, 2012). Using thermal models that describe the top-oil temperature in the transformer as a function of ambient temperature, we can then determine how much temperature rise would be expected if the climate is warmed by several degrees (Susa *et al.*, 2005; Tylavsky *et al.*, 2000). A simple thermal model is used in this analysis, given by:

$$\begin{aligned}\theta_{top} &= \theta_0 + \theta_{amb} \\ &= (\theta_u - \theta_i)(1 - \exp(-t/T_0)) + \theta_i + \theta_{amb}\end{aligned} \quad (2)$$

where θ_{top} is the top oil temperature in °C; θ_O is the initial top oil temperature in °C; θ_u is the ultimate top rise temperature for a load L in °C; θ_i is the initial top rise temperature in °C for time $t = 0$; and T_O is the time constant at rated power in hours. Equation 2 indicates that a rise in local (ambient) temperature is commensurate with a temperature rise within the transformer. Then, if all else being equal, we apply Equation 1 for a background 1˚C rise in temperature, we find that the lifetime of the transformer decreases by 4 years—or a 10% reduction. Therefore, when considering the RCP4.5 and RCP8.5 end-of-century mean global warming projections over the LPT area of ~2˚C and 4˚C respectively (IPCC, 2013—see e.g. Figure SPM.8), we can extrapolate that the mean impact on expected transformer lifetime would culminate (by end of century) to a range of 20–40%. However, as our heat wave assessment has shown, the threat from the occurrence of extreme heat events could at least double and has the potential to go up by a factor of five (under no mitigation) by the end of the century. Therefore, we must begin to consider more explicitly how more frequent heat waves could decrease the expected lifetime and incur additional costs. However, these effects are more challenging to quantify and studies (such as the aforementioned) do not explicitly account for the damaging effects of the ambient transformer environment and power demand stress from heatwaves. Nevertheless, we draw from previous analyses to present a preliminary synthesis toward a more explicit approach, which is given below.

More advanced models for transformer aging based on the hottest-oil temperature, rather than the top oil temperature, can be used as a guide to quantifying the impacts of heat waves. The main standard from IEEE is reviewed here (IEEE, 2012). We assume that Equation 2 also holds for the hottest-oil temperature since it is an analogous thermal situation to the analysis presented *vide supra*. The loss of insulation life t_{ei} in an interval t_i, based on the hottest oil temperature, Θ_H, is given for a reference temperature of 383°K as (He *et al.*, 2009; IEEE, 1996):

$$t_{ei} = t_i \exp\left(\frac{15000}{383} - \frac{15000}{\Theta_H(t_i)}\right) \quad (3)$$

Then the total loss of insulation for the transformer I_e can be calculated by summing all of the lost insulation life over an interval t_i:

$$I_e = \sum_{i=1}^{n} t_i \exp\left(\frac{15000}{383} - \frac{15000}{\Theta_H(t_i)}\right) \quad (4)$$

It can be shown that the aging failure probability P_a during an interval I_e at reference temperature Θ_O is given by (Billinton and Allan, 1992; He *et al.*, 2009):

$$P_a = \frac{F_a(I_e + \Delta t_e|\Theta_O) - F_a(I_e|\Theta_O)}{1 - F_a(I_e|\Theta_O)} \quad (5)$$

where Δt_e is the equivalent operation time. Using Equation 3 along with the definition of conditional probability (Equation 5) that a transformer will fail in an interval Δt_e after surviving T years (He *et al.*, 2009):

$$P_a = 1 - exp\left[\left(\frac{I_e}{Cexp(\frac{B}{\Theta_O})}\right)^{\beta} - \left(\frac{I_e+\Delta t_e}{Cexp(\frac{B}{\Theta_O})}\right)^{\beta}\right] \quad (6)$$

where C and β are the life parameter and shape parameter, respectively.

In cases like heat waves where the LPTs can be under duress for prolonged periods of time, the probability of failure becomes elevated, putting the electrical grid at risk. The economic impact of heat waves on LPTs can therefore be given by loss of equipment, as well as the cost of losing service to a large area of electrical customers. For the capital costs of LPTs, the prices are given in US DOE (2012) as $7,500,000 for a 750 mVA 765–138kV three phase transformer, close to what was listed in Pletka *et al.* (2014). Moreover, Lawrence Berkeley National Laboratory gives the average per event 8-hour interruption cost for residential customers, small commercial and industrial customers, and medium and large commercial and industrial customers as $17.20, $4,690 and $84,083, respectively (Sullivan *et al.*, 2015). The cost of simply repairing or replacing the transformer goes far beyond the substation walls, and has vast impacts throughout the surrounding area. Critical facilities such as hospitals, places of refuge and emergency services could also be affected, further incurring both economic and potentially human costs.

8. Summary and Discussion

In this study, we focus on how human-induced changes in climate affect heat waves that could then damage the expensive LPTs that are critical to the functioning of the electric power grid in the Northeast corridor of the United States. Methods that assess heat waves based on model simulated daily-maximum air temperature pose a challenge for assessing the potential threat or risk—as we have found a weak consensus among model simulations. We develop an analogue method for detecting the occurrence of heat wave based on the prevailing large-scale atmospheric conditions ("composites") and eschews the use of model-simulated daily maximum temperature. The composites are constructed for the summer season (JJA) of a targeted LPT location through a joint analysis of station-based daily maximum temperature observation and atmospheric reanalysis. The identified synoptic regimes demonstrate that heat waves can be predominantly associated with mid-tropospheric anticyclonic circulation, warm lower tropospheric temperature, and negative vorticity—with all features centered over the area of interest (i.e. approximate location of LPT).

We evaluate the constructed composites as a predictive analogue for heat wave. The detection diagnostics of the analogue scheme are first calibrated with 23-year (1980–2002) and then validated with 4-year (2003–2006) MERRA-2 reanalysis. The analogue scheme is found to be comparable to MERRA-2 daily maximum temperature in characterizing the number and interannual variations of observed summer heat wave days during both periods. With regard to the late 20th century (1980–2002) summer heat wave frequencies from an ensemble of CMIP5 models, heat wave frequencies based on model-simulated daily maximum temperature exhibit a weak consensus with a wide IQR and inter-model spread. In contrast, the results from the analogue scheme based on the calibrated optimal threshold values produce a more consistent multi-model median with the observation and also have substantially reduced IQR and inter- model range. This indicates that the climate models are able to reproduce the large-scale atmospheric conditions associated with heat waves with realistic frequencies.

The multi-model medians of both model-simulated daily maximum temperature and analogue scheme indicate strong decadal increases in heat wave frequency by the end of the 21st century (2070–2092) relative to the 2010–2032 period. The increases are more pronounced under the higher emission scenario (RCP8.5). The mitigation with the lower emission (RCP4.5) tends to shift the multi-model central tendency and distributions toward smaller increases, suggesting that the climate policies adopted in the coming decades will affect the occurrence of heat waves. Under both scenarios, all the models from both analyses demonstrate consistency in the sign of change (increase). However, the analogue scheme exhibits much stronger model consensus of the trend (i.e. smaller IQRs) than daily maximum temperature trend estimate.

Notably, the analogue method is implemented under the supposition that large-scale atmospheric conditions play a salient role in the occurrence of an extreme event at the local scale. Thus, alterations of small-scale processes associated with climate change that are not captured by the analogue scheme may introduce a bias in our assessment. Nevertheless, our results indicate that the analogue scheme based on "resolved" large-scale atmospheric features provides skillful assessments of the late 20th century heat wave frequencies and more consistent future changes and thus show promise as an improved and value-added diagnosis against an evaluation that considers model-simulated daily maximum temperature alone.

We showed that there are economic impacts for LPTs operating at elevated ambient temperatures, as well as during heat waves. Higher temperatures are known to degrade the insulation inside the LPTs, putting them at risk for catastrophic failure. Moreover, the degradation is cumulative, so more frequent and more intense heat waves could rapidly reduce the lifetime of an LPT, making failure more likely. Failures of LPTs have economic impacts in terms of replacement costs and impacts on the service area associated with the LPT. In this pilot study, the analogue method has been demonstrated to provide a stronger model consensus of trends in future heat wave frequency, and thus holds promise to provide a salient stride toward more reliable and actionable climate change information. In particular, for the case of assessing risks of premature failure of our nation's aging network of power transformers, they are very time consumptive and costly to replace and number in the 1,000s. Given these considerations, our future analyses will focus on expanding this analogue method for heat wave assessments to provide network coverage of the grid; identifying critical junctures/clusters in the grid at high risk; and expanding technical and econometric analyses to more explicitly account for the degrading effects and costs of extreme, episodic heatwave events on transformers (as well as other components of the grid). We see this effort as a promising step forward to not only evaluate the potential incurred damage and economic loss, but also provide actionable information for how to make the electric grid more stable, reliable, and environmentally responsible.

Acknowledgements

This work was funded by MIT Lincoln Lab (DE-FOA-0000768). We acknowledge the modeling groups, the Program for Climate Model Diagnosis and Intercomparison (PCMDI), and the WCRP's Working Group on Coupled Modeling (WGCM) for their roles in making available the WCRP CMIP5 multimodel dataset. We thank the NOAA Climate Prediction Center for the global gridded precipitation observations and the NASA Global Modeling and Assimilation Office for the MERRA Reanalysis data.

9. References

Albert, R., I. Albert & G. L. Nakarado (2004). Structural vulnerability of the North American power grid. *Phys. Rev. E*, **69**: 025103. doi:10.1103/PhysRevE.69.025103.

Askari, M.T., M.Z.A.A. Kadir, W.F.W. Ahmad & M. Izadi (2009). Investigate the effect of variations of ambient temperature on HST of transformer. *Research and Development (SCOReD),* 2009 IEEE Student Conference on, pp. 363–367. doi:10.1109/SCORED.2009.5442998.

Averyt, K., J. Fisher, A. Huber-Lee, A. Lewis, J. Macknick, N. Madden, J. Rogers & S. Tellinghuisen (2011). Freshwater use by US power plants: Electricity's thirst for a precious resource. Union of Concerned Scientists.

Barthelemy, M. (2004). Betweenness centrality in large complex networks. *The European Physical Journal B-Condensed Matter and Complex Systems*, **38**(2): 163–168.

Billinton, R. & R.N. Allan (1992). Reliability Evaluation of Engineering Systems. Springer US: New York, USA

Bompard, E., D. Wu & F. Xue (2010). The concept of betweenness in the analysis of power grid vulnerability. *Complexity in Engineering, COMPENG '10.*, pp. 52–54.

Bosilovich, M.G., R. Lucchesi & M. Suarez (2016). MERRA-2: File Specification. GMAO Office Note No. 9 (Version 1.1), 73 pp (http://gmao.gsfc.nasa.gov/pubs/office_notes).

Bromirski, P.D., N. Graham, M. Tyree & R.E. Flick (2012). Coastal flooding-potential projections: 2000–2100. CEC-500-2012-011, California Energy Commission, Scripps Institution of Oceanography (http://www.energy.ca.gov/2012publications/CEC-500-2012-011/CEC-500-2012-011.pdf).

Constable, G. & B. Somerville (eds.) (2003). *A Century of Innovation: Twenty Engineering Achievements that Transformed our Lives*. The National Academies Press: Washington, DC. (https://www.nap.edu/catalog/10726/a-century-of-innovation-twenty-engineering- achievements-that-transformed-our).

Davis, M. & S. Clemmer (2014). Power failure: how climate change puts our electricity at risk and what we can do. Union of Concerned Scientists.

Eto, J.H. (2004). *Blackout 2003: final report on the August 14, 2003 blackout in the United States and Canada: causes and recommendations.* Electricity Markets and Policy Group, Energy Analysis and Environmental Impacts Department, U.S. Department of Energy, Washington, DC.

Federal Energy Regulatory Commission (2003). Final report on price manipulation in Western markets fact-finding investigation of potential manipulation of electric and natural gas prices. (http://www.ferc.gov/legal/maj-ord-reg/land-docs/PART-I-3-26-03.pdf).

Fleischli, S. & B. Hayat (2014). Power plant cooling and associated impacts: the need to modernize US power plants and protect our water resources and aquatic ecosystems. Natural Resources Defense Council (https://www.nrdc.org/sites/default/files/power-plant-cooling-IB.pdf).

Fu, W., J.D. McCalley & V. Vittal (2001). Risk assessment for transformer loading. *IEEE Trans-actions on Power Systems*, **16**(3): 346–353.

Gao, X., C.A. Schlosser, P. Xie, E. Monier & D. Entekhabi (2014). An Analogue Approach to Identify Heavy Precipitation Events: Evaluation and Application to CMIP5 Climate Models in the United States. *J. Climate*, **27**, 5941–5963. doi:10.1175/JCLI-D-13-00598.1.

Gao, X., C.A. Schlosser, P.A. O'Gorman, E. Monier & D. Entekhabi (2017). Twenty-first-century changes in U.S. regional heavy precipitation frequency based on resolved atmospheric patterns. *J. Climate,* **30**, 2501–2521. doi:10.1175/JCLI-D-16-0544.1.

Godina, R., E.M. Rodrigues, J.C. Matias & J.P. Catalaño (2015). Effect of loads and other key factors on oil-transformer ageing: sustainability benefits and challenges. *Energies*, **8**(10): 12147–12186.

Grotjahn, R. (2011). Identifying extreme hottest days from large scale upper air data: a pilot scheme to find California Central Valley summertime maximum surface temperatures. *Climate Dynamics*, **37**(3): 587–604. doi:10.1007/s00382-011-0999-z.

He, J., Y. Sun, P. Wang & L. Cheng (2009). A hybrid conditions-dependent outage model of a transformer in reliability evaluation. *IEEE Transactions on Power Delivery*, **24**(4): 2025–2033. doi:10.1109/TPWRD.2009.2028771.

Hurricane Sandy Rebuilding Task Force (2013). Hurricane Sandy rebuilding strategy: stronger communities, a resilient region. U.S. Department of Housing and Urban Development August.

IEEE (1996). IEEE guide for loading mineral-oil-immersed transformers. *IEEE Std C57.91-1995*. doi:10.1109/IEEESTD.1996.79665.

IEEE (2012). IEEE standard test procedure for thermal evaluation of insulation systems for liquid-Immersed distribution and power transformers - redline. *IEEE Std C57.100-2011 (Revision of IEEE Std C57.100-1999) - Redline*, pp. 1–55.

Kharin, V.V., F.W. Zwiers, X. Zhang & G.C. Hegerl (2007). Changes in temperature and precipitation extremes in the IPCC ensemble of global coupled model simulations. *J. Climate*, **20**(8): 1419–1444. doi:10.1175/JCLI4066.1.

Kharin, V.V., F.W. Zwiers, X. Zhang & M. Wehner (2013). Changes in temperature and precipitation extremes in the CMIP5 ensemble. *Climatic Change*, **119**(2): 345–357.

Kinney, R., P. Crucitti, R. Albert & V. Latora (2005). Modeling cascading failures in the North American power grid. *The European Physical Journal B - Condensed Matter and Complex Systems*, **46**(1): 101–107.

Li, X., R.W. Mazur, D.R. Allen & D.R. Swatek (2005). Specifying transformer winter and summer peak-load limits. *IEEE Transactions on Power Delivery*, **20**(1): 185–190. doi:10.1109/TPWRD.2004.837680.

Lundgaard, L.E., W. Hansen, D. Linhjell & T.J. Painter (2004). Aging of oil-impregnated paper in power transformers. *IEEE Transactions on Power Delivery*, **19**(1): 230–239. doi:10.1109/TPWRD.2003.820175.

Macknick, J., R. Newmark, G. Heath & K. Hallett (2012). Operational water consumption and withdrawal factors for electricity generating technologies: a review of existing literature. *Environmental Research Letters*, **7**(4): 045802.

Meehl, G.A., C. Covey, T. Delworth, M. Latif, B. McAvaney, J.F.B. Mitchell, R.J. Stouffer & K.E. Taylor (2007). The WCRP CMIP3 multi-model dataset: A new era in climate change research. *Bull. Amer. Met. Soc.*, **88**: 1383–1394.

Melillo, J.M., T.T. Richmond & E. Yohe, GW (2014). Climate change impacts in the United States: Third National Climate Assessment. 9780160924026. U.S. Global Change Research Program U.S. Government Printing Office. doi:10.7930/J0Z31WJ2.

Menne, M.J., I. Durre, R.S. Vose, B.E. Gleason & T.G. Houston (2012). An overview of the global historical climatology network-daily database. *Journal of Atmospheric and Oceanic Technology*, **29**(7): 897–910. doi:10.1175/JTECH-D-11-00103.1.

Metwally, I.A. (2011). Failures, Monitoring and new trends of power transformers. *IEEE Potentials*, **30**(3): 36–43. doi:10.1109/MPOT.2011.940233.

Moss, R.H., J.A. Edmonds, K.A. Hibbard, M.R. Manning, S.K. Rose, D.P. van Vuuren *et al.* (2010). The next generation of scenarios for climate change research and assessment. *Nature*, **463**(7282): 747–756.

National Research Council (2003). A Century of Innovation: twenty engineering achievements that transformed our lives. The National Academies Press: Washington, DC. doi:10.17226/10726.

National Research Council (2012). Terrorism and the electric power delivery system. National Research Council. doi:10.17226/12050.

Newman, M. (2010). Networks: An Introduction. Oxford University Press, 720pp (https://books.google.com/books?id=-DgTDAAAQBAJ).

Parfomak, P.W. (2014). Physical security of the U.S. power grid: high-voltage transformer substations. Congressional Research Service, (http://fas.org/sgp/crs/homesec/R43604.pdf).

Pederson, P., D. Dudenhoeffer, S. Hartley & M. Permann (2006). Critical infrastructure interdependency modeling: a survey of US and international research. Idaho National Laboratory pp. 1–20 (http://www5vip.inl.gov/technicalpublications/Documents/3489532.pdf).

Pletka, R., J. Khangura, A. Rawlins, E. Waldren & D. Wilson (2014). Capital costs for transmission and substations: updated recommendations for WECC transmission expansion planning, Black and Veatch PROJECT NO. 181374.

President's Council of Economic Advisers, U.S. Department of Energy's Office of Electricity Delivery and Energy Reliability and The White House Office of Science and Technology (2013). Economic benefits of increasing electric grid resilience to weather outages.

Rinaldi, S. (2004). Modeling and simulating critical infrastructures and their interdependencies. *Proceedings of the 37th Hawaii International Conference on System Sciences - 2004*, pp. 1–8. doi:10.1109/HICSS.2004.1265180.

Russo, S., A. Dosio, R.G. Graversen, J. Sillmann, H. Carrao, M.B. Dunbar, A. Singleton, P. Montagna, P. Barbola & J.V. Vogt (2014). Magnitude of extreme heat waves in present climate and their projection in a warming world. *J. Geophys. Res. Atmos.*, **119**(22): 12,500–12,512.

Sathaye, J. (2011). Estimating risk to California energy infrastructure from projected climate change. *Lawrence Berkeley National Laboratory*.

Sathaye, J., L. Dale, P. Larsen, G. Fitts, K. Koy, S. Lewis & A. Lucena (2012). Estimating risk to California energy infrastructure from projected climate change. Lawrence Berkeley National Laboratory (http://www.energy.ca.gov/2012publications/CEC-500-2012-057/CEC-500-2012-057.pdf).

Schoetter, R., J. Cattiaux & H. Douville (2015). Changes of western European heat wave characteristics projected by the CMIP5 ensemble. *Climate Dynamics*, **45**(5): 1601–1616.

Select Bipartisan Committee to Investigate the Preparation for and Response to Hurricane Katrina (2006). *A failure of initiative: the final report of the select bipartisan committee to investigate the preparation for and response to hurricane Katrina.* United States House of Representatives.

Sillmann, J., V.V. Kharin, X. Zhang, F.W. Zwiers & D. Bronaugh (2013a). Climate extremes indices in the CMIP5 multimodel ensemble: Part 1. Model evaluation in the present climate. *J. Geophys. Res. Atmos.*, **118**(4): 1716–1733.

Sillmann, J., V.V. Kharin, F.W. Zwiers, X. Zhang & D. Bronaugh (2013b). Climate extremes indices in the CMIP5 multimodel ensemble: Part 2. Future climate projections. *J. Geophys. Res. Atmos.*, **118**(6): 2473–2493.

Sullivan, M.J., J. Schellenberg & M. Blundell (2015). Updated value of service reliability estimates for electric utility customers in the United States. Lawrence Berkeley National Laboratory.

Susa, D. & H. Nordman (2009). A simple model for calculating transformer hot-spot temperature. *IEEE Transactions on Power Delivery*, **24**(3): 1257–1265. doi:10.1109/TPWRD.2009.2022670.

Susa, D., M. Lehtonen & H. Nordman (2005). Dynamic thermal modelling of power transformers. *IEEE Transactions on Power Delivery*, **20**(1): 197–204. doi:10.1109/TPWRD.2004.835255.

Taylor, K.E., R.J. Stouffer & G.A. Meehl (2011). An overview of CMIP5 and the experiment design. *Bull. Amer. Meteor. Soc.*, **93**(4): 485–498. doi:10.1175/BAMS-D-11-00094.1.

The Electric Power Research Institute (2014). Considerations for a power transformer emergency spare strategy for the electric utility industry.

Tylavsky, D.J., Q. He, J. Si, G.A. McCulla & J.R. Hunt (2000). Transformer top-oil temperature modeling and simulation. *IEEE Transactions on Industry Applications*, **36**(5): 1219–1225. doi:10.1109/28.871267.

United States Government Accountability Office (2014). Climate change - Energy infrastructure risks and adaptation efforts.

US DOE (2012). Large power transformers and the U.S. electric grid. 55 p.

US DOE (2015). Enabling modernization of the electric power system. In: Quadrennial Technology Review, United States Department of Energy, Chapter 3, 22 p.

van Vliet, M.T.H., J.R. Yearsley, F. Ludwig, S. Vogele, D.P. Lettenmaier & P. Kabat (2012). Vulnerability of US and European electricity supply to climate change. *Nature Climate Change*, **2**(9): 676–681.

Weekes, T., T. Molinski, X. Li & G. Swift (2004). Risk assessment using transformer loss of life data. *IEEE Electrical Insulation Magazine*, **20**(2): 27–31. doi:10.1109/MEI.2004.1283259.

Williams, M.D., S.L. Goodrick, A. Grundstein & M. Shepherd (2015). Comparison of dew point temperature estimation methods in Southwestern Georgia. *Physical Geography*, **36**(4): 255–267. doi:10.1080/02723646.2015.1011554.

Zamuda, C., B. Mignone, D. Bilello, K. Hallett, C. Lee, J. Macknick, R. Newmark & D. Steinberg (2013). US energy sector vulnerabilities to climate change and extreme weather. U.S. Department of Energy's Office of Policy and International Affairs and the National Renewable Energy Laboratory.

Joint Program Report Series - Recent Articles

For limited quantities, Joint Program Reports are available free of charge. Contact the Joint Program Office to order.
Complete list: http://globalchange.mit.edu/publications

317. **Application of the Analogue Method to Modeling Heat Waves: A Case Study With Power Transformers.** *Gao et al., Aug 2017*
316. **The Revenue Implications of a Carbon Tax.** *Yuan et al., Jul 2017*
315. **The Future Water Risks Under Global Change in Southern and Eastern Asia: Implications of Mitigation.** *Gao et al., Jul 2017*
314. **Modeling the Income Dependence of Household Energy Consumption and its Implications for Climate Policy in China.** *Caron et al., Jul 2017*
313. **Global economic growth and agricultural land conversion under uncertain productivity improvements in agriculture.** *Lanz et al., Jun 2017*
312. **Can Tariffs be Used to Enforce Paris Climate Commitments?** *Winchester, Jun 2017*
311. **A Review of and Perspectives on Global Change Modeling for Northern Eurasia.** *Monier et al., May 2017*
310. **The Future of Coal in China.** *Zhang et al., Apr 2017*
309. **Climate Stabilization at 2°C and Net Zero Carbon Emissions.** *Sokolov et al., Mar 2017*
308. **Transparency in the Paris Agreement.** *Jacoby et al., Feb 2017*
307. **Economic Projection with Non-homothetic Preferences: The Performance and Application of a CDE Demand System.** *Chen, Dec 2016*
306. **A Drought Indicator based on Ecosystem Responses to Water Availability: The Normalized Ecosystem Drought Index.** *Chang et al., Nov 2016*
305. **Is Current Irrigation Sustainable in the United States? An Integrated Assessment of Climate Change Impact on Water Resources and Irrigated Crop Yields.** *Blanc et al., Nov 2016*
304. **The Impact of Oil Prices on Bioenergy, Emissions and Land Use.** *Winchester & Ledvina, Oct 2016*
303. **Scaling Compliance with Coverage? Firm-level Performance in China's Industrial Energy Conservation Program.** *Karplus et al., Oct 2016*
302. **21st Century Changes in U.S. Heavy Precipitation Frequency Based on Resolved Atmospheric Patterns.** *Gao et al., Oct 2016*
301. **Combining Price and Quantity Controls under Partitioned Environmental Regulation.** *Abrell & Rausch, Jul 2016*
300. **The Impact of Water Scarcity on Food, Bioenergy and Deforestation.** *Winchester et al., Jul 2016*
299. **The Impact of Coordinated Policies on Air Pollution Emissions from Road Transportation in China.** *Kishimoto et al., Jun 2016*
298. **Modeling Regional Carbon Dioxide Flux over California using the WRF-ACASA Coupled Model.** *Xu et al., Jun 2016*
297. **Electricity Investments under Technology Cost Uncertainty and Stochastic Technological Learning.** *Morris et al., May 2016*
296. **Statistical Emulators of Maize, Rice, Soybean and Wheat Yields from Global Gridded Crop Models.** *Blanc, May 2016*
295. **Are Land-use Emissions Scalable with Increasing Corn Ethanol Mandates in the United States?** *Ejaz et al., Apr 2016*
294. **The Future of Natural Gas in China: Effects of Pricing Reform and Climate Policy.** *Zhang & Paltsev, Mar 2016*
293. **Uncertainty in Future Agro-Climate Projections in the United States and Benefits of Greenhouse Gas Mitigation.** *Monier et al., Mar 2016*
292. **Costs of Climate Mitigation Policies.** *Chen et al., Mar 2016*
291. **Scenarios of Global Change: Integrated Assessment of Climate Impacts.** *Paltsev et al., Feb 2016*
290. **Modeling Uncertainty in Climate Change: A Multi-Model Comparison.** *Gillingham et al., Dec 2015*
289. **The Impact of Climate Policy on Carbon Capture and Storage Deployment in China.** *Zhang et al., Dec 2015*
288. **The Influence of Gas-to-Liquids and Natural Gas Production Technology Penetration on the Crude Oil-Natural Gas Price Relationship.** *Ramberg et al., Dec 2015*
287. **Impact of Canopy Representations on Regional Modeling of Evapotranspiration using the WRF-ACASA Coupled Model.** *Xu et al., Dec 2015*
286. **Launching a New Climate Regime.** *Jacoby & Chen, Nov 2015*
285. **US Major Crops' Uncertain Climate Change Risks and Greenhouse Gas Mitigation Benefits.** *Sue Wing et al., Oct 2015*
284. **Capturing Natural Resource Dynamics in Top-Down Energy-Economic Equilibrium Models.** *Zhang et al., Oct 2015*
283. **Global population growth, technology, and Malthusian constraints: A quantitative growth theoretic perspective.** *Lanz et al., Oct 2015*
282. **Natural Gas Pricing Reform in China: Getting Closer to a Market System?** *Paltsev & Zhang, Jul 2015*
281. **Impacts of CO_2 Mandates for New Cars in the European Union.** *Paltsev et al., May 2015*

MIT Joint Program on the Science and Policy of Global Change

Massachusetts Institute of Technology
77 Massachusetts Ave., E19-411
Cambridge MA 02139-4307 (USA)

T (617) 253-7492 **F** (617) 253-9845
globalchange@mit.edu
http://globalchange.mit.edu/